

Characterization of the BNNO Radical

Qianyi Cheng, Andrew C. Simmonett, Francesco A. Evangelista, Yukio Yamaguchi,
and Henry F. Schaefer III*

*Center for Computational Quantum Chemistry, 1004 Cedar Street, University of
Georgia, Athens, Georgia 30602*

Received March 8, 2010

Abstract: The cyclic, trans, and cis BNNO molecules and the two isomerization reactions on their doublet electronic states potential energy surface (PES) are systematically investigated. Ab initio self-consistent field, complete active space self-consistent field, coupled cluster with single and double excitations (CCSD), and CCSD including perturbative triple excitations [CCSD(T)] quantum mechanical techniques are employed, in conjunction with Dunning's correlation consistent polarized valence basis sets (cc-pVXZ and aug-cc-pVXZ, where X = D, T, and Q). All stationary points located on the doublet PES lie within 19 kcal mol⁻¹ of the global minimum cyclic isomer at the aug-cc-pVQZ CCSD(T) level of theory. The cyclic and trans minima are separated by 2.4 kcal mol⁻¹ with an interconversion barrier (cyclic → TS2 → trans) of 18.3 kcal mol⁻¹; the trans and cis isomers are separated by 10.4 kcal mol⁻¹ with a barrier (trans → TS1 → cis) of 10.4 kcal mol⁻¹. The dissociation energies BNNO (\tilde{X}^2A') → B (2P_u) + NNO ($\tilde{X}^1\Sigma^+$) for the cyclic, trans, and cis isomers are predicted to be 39.7, 37.3, and 27.0 kcal mol⁻¹, respectively. The diatomic fragment dissociation energies BNNO (\tilde{X}^2A') → BN ($X^3\Pi$) + NO ($X^2\Sigma^+$) for the three isomers are determined to be 50.7, 48.4, and 38.0 kcal mol⁻¹, respectively. Additionally, fundamental vibrational frequencies are computed for the cyclic and trans isomers through application of second-order vibrational perturbation theory (VPT2) at the cc-pCVTZ CCSD(T) level of theory. Comparison of the resulting vibrational frequencies and their isotopic shifts with those determined experimentally by Wang and Zhou yields the surprising result that the B (2P_u) + NNO ($\tilde{X}^1\Sigma^+$) reaction leads to formation of the trans isomer. The latter structure is not the global minimum, rather the second lowest lying isomer. This apparent disparity is rationalized by detailed examination of the PES describing this reaction.

Introduction

In the past few decades, boron nitrides have attracted much attention since they have various technical applications in nuclear technology and in the semiconductor and steel industries, taking advantage of their mechanical, thermal, and electrical properties as well as their chemical inertness.^{1,2} For the amount of energy stored in a given system or region of space per unit volume, or per unit mass, boron is well-known for its high energetic density, among many kinds of propellant additives.³ Therefore, boron has potential applications as an advanced fuel in propulsion systems.⁴ During the burning of boron-containing propellants, some portions

of boron are oxidized to boron oxide releasing a large amount of energy, while some boron nitride (BN) is formed.^{5,6}

As an important molecule in atmospheric chemistry, nitrous oxide (N₂O) has also received considerable attention and interest. In the chemical industry, nitrous oxide is an effective oxidation agent.^{7–23} Many experiments indicate that nitrous oxide is also important in the thermal decomposition of various propellants.³ N₂O is often used as a catalytic species for burn-rate modification of nitramine propellants as well.^{24,25}

The reaction of boron and nitrous oxides and the resulting intermediate generation is an intriguing topic. In 2007, Wang and Zhou reported a combined matrix isolation infrared (IR) spectroscopic and theoretical study of the BNNO and AINNO

* E-mail: sch@uga.edu.

molecules.²⁶ The BNNO and AlNNO molecules were prepared via the reactions of laser-evaporated boron and aluminum atoms with nitrous oxide (N₂O) in solid argon and were identified on the basis of isotopically substituted IR absorptions as well as theoretical (density functional theory) calculations. From codeposition of laser-evaporated isotopic-enriched ¹⁰B atoms with 0.5% N₂O in argon matrix, a group of new IR absorptions at 1837.0, 1502.3, 838.2, and 633.8 cm⁻¹ were observed, along with strong N₂O absorptions. These four absorptions were assigned to the B–N stretching (1837.0 cm⁻¹), N–O stretching (1502.3 cm⁻¹), N–N stretching (838.2 cm⁻¹), and in-plane bending (633.8 cm⁻¹) modes of the ¹⁰BNNO molecule.²⁶ The experiment was repeated with naturally abundant boron atoms, yielding absorptions at 1795.7, 1500.3, 836.5, and 626.9 cm⁻¹ with IR intensities approximately four times stronger than the above-mentioned absorptions. The latter vibrational features were assigned to the corresponding modes of the ¹¹BNNO molecule. In order to confirm their findings, Wang and Zhou carried out B3LYP density functional theory (DFT) computations with the 6-311+G* basis set; the BNNO molecule was predicted to have a ²A' ground electronic state with a planar trans structure.

Wang, Li, Zhang, Sheng, and Yu reported a theoretical study of boron nitride (BN) generated from the boron atom and several nitrogen oxides.³ BN is one of the products formed in the burning of a boron-containing propellant. Possible mechanisms for the reactions of boron and nitrogen oxides (NO, NO₂, and N₂O) were investigated using the G2-MP2 method. The reactions of the ground-state boron atom B (²P_u) with nitrogen oxides were determined to be endothermic, while the reactions of an excited quartet state of the boron atom B (⁴P_g) and nitrogen oxides are exothermic, and the BN product can be formed. For the BN formation reaction B (⁴P_g) + N₂O → BN + NO, two trans and two cis forms of the BNNO molecule were located on the quartet potential energy surface (PES). Among the four, one trans and one cis form were found as the reaction intermediates, and the other trans and cis BNNO structures were characterized as transition states from the intermediates to the final products (BN + NO).

In this study we make the first attempt to theoretically interpret the experimentally observed vibrational frequencies by explicitly considering the effects of anharmonicity. Furthermore, we extend the previous studies of the PES by employing significantly more reliable methodologies and reveal a previously neglected isomer which, surprisingly, is revealed to be the global minimum.

Theoretical Methods

In this work, six correlation-consistent basis sets cc-pVXZ and aug-cc-pVXZ, where X = D, T, and Q, developed by Dunning and co-workers^{27,28} were employed. Ab initio theoretical techniques included restricted open-shell Hartree–Fock (ROHF), unrestricted Hartree–Fock (UHF), complete active space self-consistent field (CASSCF),^{29,30} spin-unrestricted coupled cluster with single and double excitations (UCCSD),^{31,32} and UCCSD with perturbative triple excitations [UCCSD(T)].^{33–35} For the unrestricted

coupled cluster computations, an ROHF reference wave function was used to control spin contamination. Computations were performed with the Molpro program suite,³⁶ the Mainz–Austin–Budapest (MAB) version of the ACESII program suite,^{37,38} and PSI3³⁹ quantum chemistry packages.

The four core orbitals (1s-like orbitals of B, N, and O) were frozen in all correlated calculations. The *T*₁ diagnostic values⁴⁰ of the five stationary points are 0.027 (cyclic isomer), 0.022 (trans isomer), 0.035 (cis isomer), 0.032 (TS1), and 0.034 (TS2) at the cc-pVQZ UCCSD(T) optimized geometries. Analytic and numerical gradient methods were used to optimize geometries and to determine the dipole moments, harmonic vibrational frequencies, and associated IR intensities. Vibrational anharmonicities were computed by application of second-order perturbation theory^{41–48} (VPT2) to the quartic force field. The Grendel⁴⁹ program was used to compute the force constants in internal coordinates, while Intder2005^{50–54} was used to perform the nonlinear transformation of the force constants from the internal to Cartesian coordinates. The Anharm^{53,55} program was adopted for the VPT2 analysis.

Results and Discussion

A. CASSCF Wave Functions. The electron configurations of the linear NNO ($\tilde{X}^1\Sigma^+$) and the cyclic, trans, and cis BNNO isomers as well as the two isomerization reaction transition states (TS1 and TS2) connecting them are shown in the Supporting Information, Table S1. The five highest-lying occupied molecular orbitals (MO) of the five stationary points of BNNO molecule and the linear NNO molecule are depicted in the Supporting Information, Figures S1–S6.⁵⁷

In order to analyze correlation effects on the geometrical parameters and physical properties, full valence (19e/16MO) cc-pVQZ CASSCF wave functions were constructed for the five stationary points at the cc-pVQZ UCCSD(T) optimized geometries. There are 17 705 688 configuration state functions (CSFs) in *C_s* point group symmetry. Furthermore, since multireference character might be present, given the moderately large *T*₁ diagnostics, we will examine the contributions of the reference wave function and the important excited configurations. Therefore, the CI coefficients based on natural orbitals (NOs), presented in the Supporting Information, Table S2, are employed in the following discussion.

For cyclic BNNO, the (2*a*'')² → (3*a*'')² double excitation provides the most significant correction to the reference configuration. For trans BNNO, the three most significant contributions to the CASSCF wave function come from the (2*a*'')² → (3*a*'')², (11*a*')² → (13*a*')², and (1*a*'')² → (4*a*'')² double excitations relative to the reference configuration. A major contribution to the CASSCF wave function for the cis isomer comes from the (13*a*)² → (15*a*)² double excitation. Similar to the cis isomer, the primary contribution to the CASSCF wave function of TS1 comes from the (13*a*)² → (15*a*)² double excitation, and the two important additional contributions are the (12*a*)² → (16*a*)² and (11*a*)(13*a*) → (14*a*)(15*a*) double excitations. It should be noted that the CI coefficient of the reference configuration for the TS1 transition state (*C*₁ = 0.912) is the same as the cis isomer

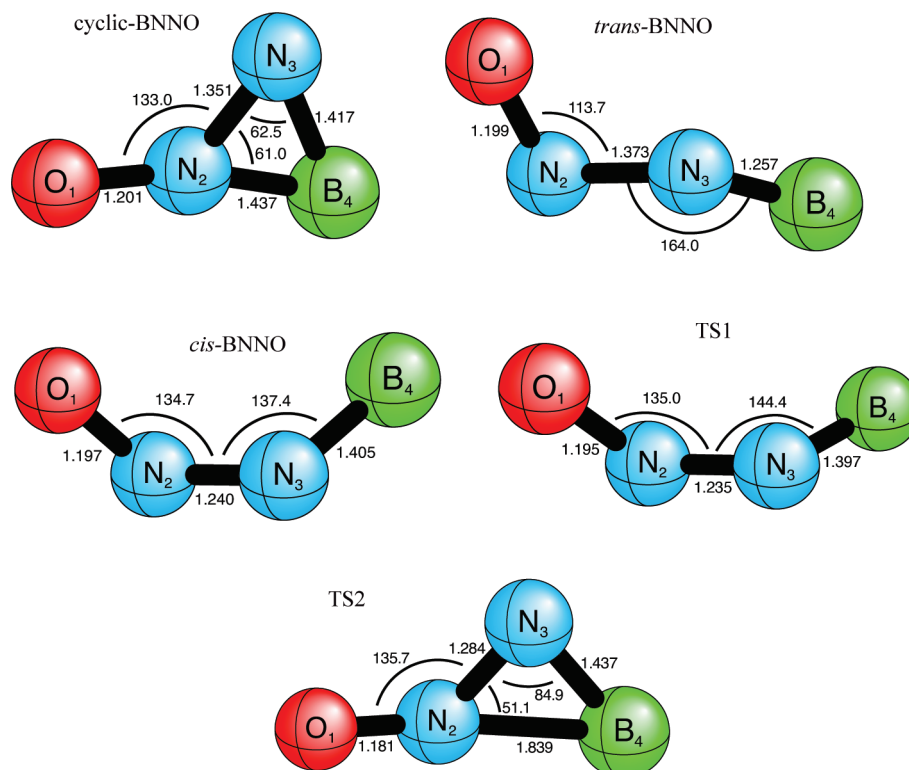


Figure 1. The optimized geometries (Å and °) of the five stationary point structures of BNNO at the aug-cc-pVQZ CCSD(T) level of theory. τ (BNNO) for the cis BNNO isomer is 38.8°, and τ for TS1 is 80.4°. The TS1 geometrical parameters are at the cc-pVQZ CCSD(T) level of theory.

but smaller than those for the cyclic and trans isomers. For TS2, three important double excitations, $(2a'')^2 \rightarrow (3a'')^2$, $(11a')^2(12a') \rightarrow (11a')(12a')(13a')$, and $(11a')^2 \rightarrow (13a')^2$ contribute to the CASSCF wave function. The CI coefficient of the reference configuration for the TS2 transition state ($C_1 = 0.914$) is smaller than those of the cyclic and trans isomers, as a result of the elongated bonds in the transition state. Despite the significant presence of some excited configurations, the reference CI coefficients should be large enough in all cases for the single reference coupled cluster theory to be reliable.

B. Geometries. The optimized geometries for the five stationary points of the BNNO molecule are presented in Figure 1 and the Supporting Information, Table S3. In the following discussion we used the most reliable aug-cc-pVQZ CCSD(T) geometries for all species, with the exception of TS1, for which we encountered difficulties. Notwithstanding the change (0.5°) in θ_e (BNN) for the cis isomer, which has a very flat potential surface, it is evident from the Supporting Information, Table S3 that the aug-cc-pVQZ and cc-pVQZ geometries are nearly identical. In part for this reason, it was decided not to further pursue the aug-cc-pVQZ CCSD(T) geometry for TS1; instead we performed a single-point energy computation at this level of theory using the cc-pVQZ CCSD(T) geometry, anticipating negligible error in the resulting barrier height.

The r_e (BN) bond distances in the five stationary points of the BNNO molecule are all predicted to be 1.417–1.437 Å, except for the trans minimum. These 1.4 Å values are very close to those of the boron- and nitrogen-containing three-membered rings from Richard and Ball's theoretical work⁵⁸

[1.410 Å for both trans and cis diazaboridine and 1.420 Å for boradiazirine computed at the 6-31G(d,p) B3LYP level], in which B–N is a single bond. The trans BNNO isomer has the shortest BN-bond distance of 1.257 Å, which may be attributed to the two BN π -bonding (out-of-plane $2a''$ and in-plane $11a'$ MO) orbitals shown in the Supporting Information, Figure S2. This bond length is shorter than those for BN ($X^3\Pi$) (1.330 Å), which is considered to have the character between a double and a triple bond, and BN ($a^1\Sigma^+$) (1.277 Å),⁵⁹ which is considered as a triple bond.

The N–N bond distances of the cyclic and trans minima are 1.351 and 1.373 Å, respectively, much longer than those of isolated nitrous oxide (N–N triple bond⁵⁶ 1.129 Å) and diazene (N–N double bond 1.252 Å), much shorter than those of cis diazaboridine (1.585 Å)⁵⁸ and hydrazine (1.460 Å),⁶⁰ and close to that predicted for boradiazirine (1.300 Å)⁵⁸ at the B3LYP 6-31G(d,p) level. Therefore, the NN bonds in the cyclic and trans isomers fall between single and double bonds. For the cis minimum and the TS1 transition state, the N–N bond lengths are very close to diazene.

All of the O–N bond distances fall in the range 1.181–1.201 Å for the five stationary points. These values are much longer than that for ($X^2\Pi$) diatomic nitric oxide (1.153 Å). Except for TS2, the O–N bond distances of the other four stationary points are also slightly longer than that for N₂O (1.188 Å).

The equilibrium bond angle θ_e (BNN) of the trans isomer is predicted to be the largest, around 164°, which suggests near sp hybridization for the B and N atoms. On the other hand, the bond angle θ_e (NNO) of the trans isomer is determined to be the smallest among the five stationary

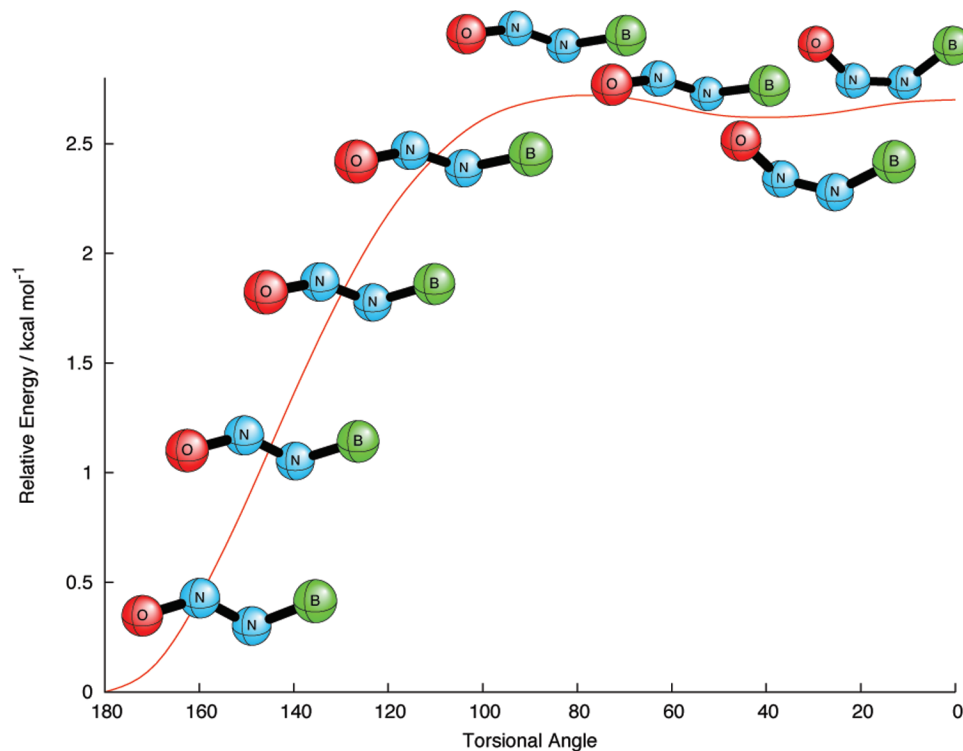


Figure 2. Relaxed potential energy curve for BNNO, plotted as a function of the torsional angle τ (BNNO), at the cc-pVTZ CCSD(T) level of theory.

points, about 114° , indicating something between sp^2 and sp^3 N and O hybridization. For the cis isomer, the bond angles θ_e (BNN) and θ_e (NNO) are predicted to be 137.4° and 134.7° , respectively. These geometrical features indicate a combination of sp and sp^2 hybridization for the B and N atoms and the same type of hybridization for the O and N atoms in the cis isomer.

C. Intrinsic Reaction Coordinate (IRC). Intrinsic reaction coordinate (IRC) analyses^{61–64} are commonly used to ascertain the nature of transition states; this requires locating a reaction coordinate, which is achieved by following appropriately mass-weighted energy gradients. The torsional motion that connects the cis and trans BNNO isomers has an extremely flat potential in the vicinity of the transition states, as exemplified by the small cis BNNO–TS1 separation of just $0.06 \text{ kcal mol}^{-1}$; this makes gradient-following algorithms susceptible to numerical error. Instead, we manually varied the torsional angle, which is the primary contributor to the reaction coordinate, relaxing all other degrees of freedom to construct a potential energy curve at the cc-pVTZ CCSD(T) level of theory. This analysis, which is displayed in Figure 2, shows that the cis isomer does not reside in a deep enough potential well to be feasibly isolable and that its formation would immediately be followed by isomerization to trans BNNO. The region of Figure 2 around the C_1 cis BNNO minimum reveals that equilibrium structure of this isomer is ill-defined, as isomerization between the two equivalent C_1 minima occurs through a C_s symmetry transition state that is almost isoenergetic.

The transition state connecting the cyclic and trans BNNO minima is much more well-defined, and its cc-pVDZ MP2 IRC is plotted in Figure 3. For the forward reaction (cyclic \rightarrow TS2 \rightarrow trans), the BN_3N_2 bond angle (see Figure 1 for

atom numbering) of the cyclic isomer gradually opens up and the NN bond distance decreases toward TS2. At the transition state, the BN_2 bond distance [1.839 \AA with the aug-cc-pVQZ CCSD(T) method] is significantly elongated compared to that (1.437 \AA with the same method) of the cyclic isomer. From the transition state (TS2) to the trans isomer, there is a cleavage of the BN_2 bond, followed by shortening of the BN_3 bond distance.

D. Relative Energies. The relative energies of the five stationary points are presented in Table 1. At the SCF level of theory, the trans isomer is predicted to be the energetically lowest-lying isomer. However, at the coupled cluster levels of theory, the cyclic isomer is found to be the global minimum on the ground-state surface. With the aug-cc-pVQZ CCSD(T) method, the trans BNNO structure is predicted to be higher in energy than the cyclic minimum, by $3.5 \text{ kcal mol}^{-1}$ [$2.4 \text{ kcal mol}^{-1}$ with zero-point vibrational energy (ZPVE) correction], but lower in energy than the cis isomer by $10.6 \text{ kcal mol}^{-1}$ ($10.4 \text{ kcal mol}^{-1}$ with ZPVE). The schematic PES at this level is shown in Figure 4.

The barrier height for the forward cyclic–trans isomerization reaction (cyclic \rightarrow TS2 \rightarrow trans) is determined to be $19.7 \text{ kcal mol}^{-1}$ ($18.3 \text{ kcal mol}^{-1}$ with ZPVE), while the reaction barrier for the reverse reaction (trans \rightarrow TS2 \rightarrow cyclic) is predicted to be $16.2 \text{ kcal mol}^{-1}$ ($15.9 \text{ kcal mol}^{-1}$ with ZPVE). Since the isomerization barrier heights are relatively high, the reaction may not happen at an appreciable rate in an argon matrix at 12K and would be highly dependent upon boron tunneling. This cyclic–trans isomerization reaction will be addressed again later in the manuscript.

The reaction barrier for the forward trans rotational (out-of-plane) isomerization reaction (trans \rightarrow TS1 \rightarrow cis) was predicted to be 10.8 (10.4) kcal mol^{-1} . On the other hand,

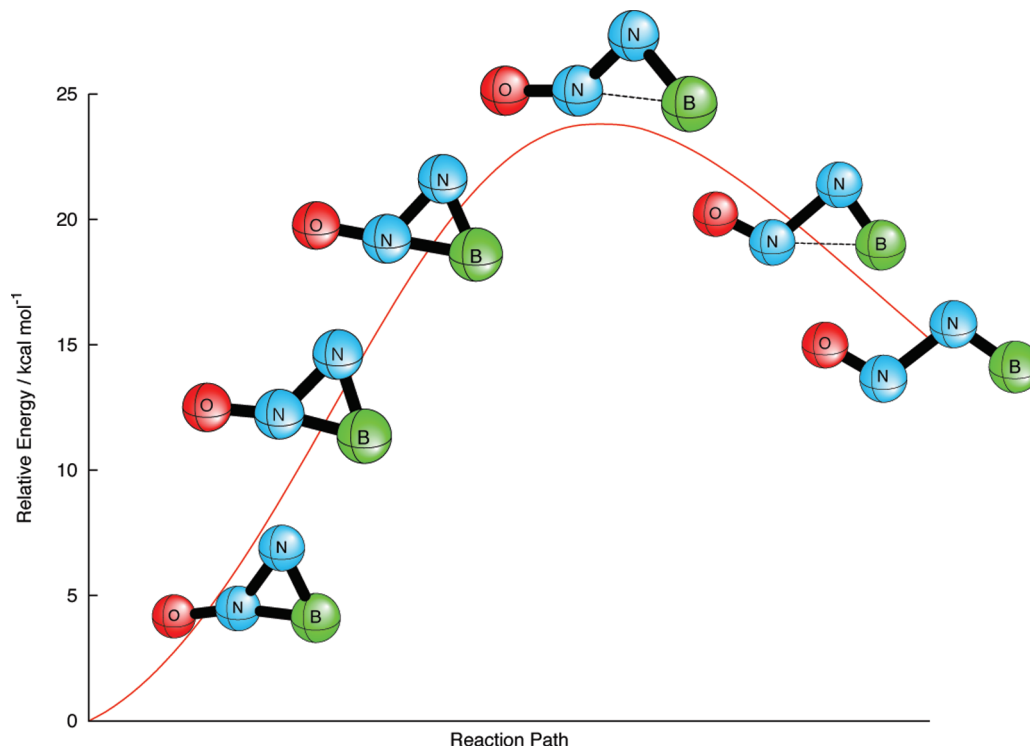


Figure 3. Intrinsic reaction coordinate (IRC) for the cyclic–trans isomerization reaction of BNNO at the cc-pVDZ MP2 level of theory.

Table 1. Relative Energies of Five Stationary Points on the PES for the BNNO Molecule at SCF, CCSD, and CCSD(T) Levels of Theory^a

| level of theory | cyclic | trans | cis | TS1 | TS2 |
|---------------------|-------------|---------------|---------------|----------------------------|---------------|
| cc-pVTZ SCF | 0.00 (0.00) | −3.76 (−4.61) | 17.94 (16.50) | 19.50 (17.55) | 18.43 (16.64) |
| aug-cc-pVTZ SCF | 0.00 (0.00) | −3.35 (−4.19) | 18.67 (17.22) | 20.22 (18.25) | 18.49 (16.70) |
| cc-pVQZ SCF | 0.00 (0.00) | −3.59 (−4.44) | 18.58 (17.13) | 20.11 (18.14) | 18.51 (16.72) |
| aug-cc-pVQZ SCF | 0.00 (0.00) | −3.48 (−4.34) | 18.76 (17.31) | 20.28 (18.31) | 18.54 (16.75) |
| cc-pVTZ CCSD | 0.00 (0.00) | 1.11 (0.15) | 13.34 (11.50) | 13.80 (12.31) | 19.04 (17.14) |
| aug-cc-pVTZ CCSD | 0.00 (0.00) | 1.52 (0.58) | 14.11 (12.24) | 14.60 (13.10) | 19.56 (17.66) |
| cc-pVQZ CCSD | 0.00 (0.00) | 1.48 (0.52) | 14.64 (12.76) | 15.09 (13.57) | 20.21 (18.29) |
| aug-cc-pVQZ CCSD | 0.00 (0.00) | 1.52 (0.58) | 14.84 (12.96) | 15.30 (13.79) | 20.38 (18.47) |
| cc-pVTZ CCSD(T) | 0.00 (0.00) | 3.22 (1.82) | 12.81 (11.42) | 12.91 (11.54) | 18.49 (17.04) |
| aug-cc-pVTZ CCSD(T) | 0.00 (0.00) | 3.50 (2.33) | 13.44 (12.00) | 13.57 (12.16) | 18.97 (17.53) |
| cc-pVQZ CCSD(T) | 0.00 (0.00) | 3.51 (2.33) | 13.96 (12.61) | 14.09 (12.65) | 19.57 (18.09) |
| aug-cc-pVQZ CCSD(T) | 0.00 (0.00) | 3.50 (2.35) | 14.10 (12.76) | 14.25 (12.82) ^b | 19.74 (18.27) |

^a Relative energies are in kcal mol^{−1}. ZPVE corrected values are in parentheses. ^b ZPVE values computed at the cc-pVQZ CCSD(T) level of theory.

there is almost no barrier [0.2 kcal mol^{−1} (0.0 kcal mol^{−1} with ZPVE correction)] for the reverse isomerization reaction (cis → TS1 → trans). Consequently, the existence of the cis isomer in a solid argon matrix (at 12K) seems questionable.

E. Dissociation Energies. The two BNNO dissociation limits at the aug-cc-pVQZ CCSD(T) level of theory are shown schematically in Figure 4.

1. $\text{BNNO } (\tilde{X}^2A') \rightarrow \text{B } ({}^2P_u) + \text{NNO } (\tilde{X}^1\Sigma^+)$. The dissociation energies $\text{BNNO } (\tilde{X}^2A') \rightarrow \text{B } ({}^2P_u) + \text{NNO } (\tilde{X}^1\Sigma^+)$ for the three BNNO isomers are presented in Table 2. With the aug-cc-pVQZ basis set the dissociation energy (ZPVE corrected values in parentheses) for the cyclic minimum is predicted to be 30.5 (28.5) (SCF), 38.3 (36.2) (CCSD), and 41.3 (39.7) kcal mol^{−1} [CCSD(T)]. For the trans isomer, the three corresponding values are 34.0 (32.8) (SCF), 36.8 (35.6) (CCSD), and 37.8 (37.3) kcal mol^{−1}

[CCSD(T)], while those for the cis isomer are 11.9 (11.3) (SCF), 23.6 (23.4) (CCSD), and 27.3 (27.0) kcal mol^{−1} [CCSD(T)]. With inclusion of correlation effects, the dissociation energies increase relative to the SCF method by 11.2 (cyclic), 4.5 (trans), and 15.7 (cis) kcal mol^{−1}, respectively. The cis isomer is more favored energetically by correlation effects compared those of the two dissociation products. It is seen that the $\text{B } ({}^2P_u) + \text{NNO } (\tilde{X}^1\Sigma^+)$ dissociation pathways are endothermic for all three BNNO isomers (see Figure 4).

2. $\text{BNNO } (\tilde{X}^2A') \rightarrow \text{BN } (X^3\Pi) + \text{NO } (X^2\Sigma^+)$. The dissociation energies $\text{BNNO } (\tilde{X}^2A') \rightarrow \text{BN } (X^3\Pi) + \text{NO } (X^2\Sigma^+)$ for the three BNNO isomers are reported in Table 2. The dissociation energy with the ZPVE correction for the cyclic minimum is 13.6 (SCF), 44.6 (CCSD), and 50.7 kcal mol^{−1} [CCSD(T)]. For the trans isomer, the dissociation

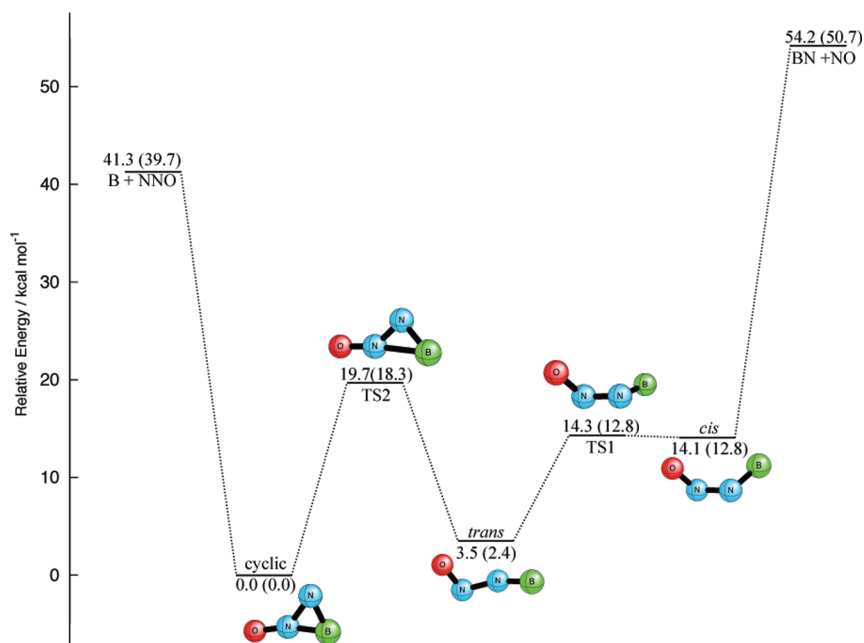


Figure 4. Stationary points on the BNNO PES at the aug-cc-pVQZ CCSD(T) level of theory. Relative energies are in kcal mol⁻¹ (ZPVE corrected values in parentheses).

Table 2. Dissociation Energies of the BNNO (\tilde{X}^2A') \rightarrow B (2P_u) + NNO ($\tilde{X}^1\Sigma^+$) and BNNO (\tilde{X}^2A') \rightarrow BN ($X^3\Pi$) + NO ($X^2\Sigma^+$) Channels at the SCF, CCSD, and CCSD(T) Levels of Theory with the aug-cc-pVQZ Basis Set^a

| level of theory | cyclic | trans | cis |
|--|---------------|---------------|---------------|
| BNNO (\tilde{X}^2A') \rightarrow B (2P_u) + NNO ($\tilde{X}^1\Sigma^+$) | | | |
| aug-cc-pVQZ SCF | 30.50 (28.45) | 33.95 (32.75) | 11.91 (11.32) |
| aug-cc-pVQZ CCSD | 38.27 (36.17) | 36.77 (35.60) | 23.58 (23.35) |
| aug-cc-pVQZ CCSD(T) | 41.27 (39.65) | 37.81 (37.33) | 27.30 (27.02) |
| BNNO (\tilde{X}^2A') \rightarrow BN ($X^3\Pi$) + NO ($X^2\Sigma^+$) | | | |
| aug-cc-pVQZ SCF | 17.58 (13.55) | 21.03 (17.86) | -1.00 (-3.57) |
| aug-cc-pVQZ CCSD | 48.34 (44.61) | 46.84 (44.04) | 33.65 (31.79) |
| aug-cc-pVQZ CCSD(T) | 54.22 (50.67) | 50.75 (48.35) | 40.25 (38.04) |

^a Dissociation energies in kcal mol⁻¹ and ZPVE corrected values are in parentheses.

energy is determined to be 17.9 (SCF), 44.0 (CCSD), and 48.4 kcal mol⁻¹ [CCSD(T)], whereas that for the cis isomer is -3.6 (SCF), 31.8 (CCSD), and 38.0 kcal mol⁻¹ [CCSD(T)] with the aug-cc-pVQZ basis set. For the three equilibrium structures, the increases of the dissociation energies with inclusion of correlation effects are 37.1 (cyclic), 30.5 (trans), and 41.6 (cis) kcal mol⁻¹, respectively. These BN ($X^3\Pi$) + NO ($X^2\Sigma^+$) dissociation reactions are thermodynamically disfavored relative to the B (2P_u) + NNO ($\tilde{X}^1\Sigma^+$) pathway discussed above (see Figure 4).

F. Dipole Moments. The dipole moments for the five stationary points are presented in the Supporting Information, Tables S6–S10. For the three equilibrium structures, the dipole moments are predicted to be 1.90 (cyclic), 2.27 (trans), and 1.16 (cis) debye at the aug-cc-pVTZ CCSD(T) (CCSD for cis) level of theory. The trans isomer has the largest dipole moment, with the expected sign ⁺BNNO⁻.

G. Harmonic Vibrational Frequencies. The harmonic vibrational frequencies for the five stationary points of the BNNO molecule at the aug-cc-pVQZ CCSD(T) level of theory are reported in Table 3 and in the Supporting Information, Tables S6–S10. The four-highest frequencies

are predicted to be 1712, 1298, 1013, and 859 cm⁻¹ for the cyclic minimum and 1876, 1544, 874, and 646 cm⁻¹ for the trans isomer, while they are 1641, 1368, 1011, and 679 cm⁻¹ for the cis isomer.

The corresponding experimentally observed (fundamental) frequencies are 1795.7, 1500.3, 836.5, and 626.9 cm⁻¹ for the ¹¹BNNO isotopologue.⁶⁵ Among three isomers, four vibrational frequencies of the ¹¹BNNO isotopologue for the trans isomer are most consistent with Wang and Zhou's experimental values. A more detailed comparison of the theoretical fundamental frequencies with Wang and Zhou's experimental observations will be given in Section I.

H. Infrared (IR) Intensities. The IR intensities of the six vibrational modes for three equilibrium isomers are presented in the Supporting Information, Tables S6–S10. From the IR spectra of Wang and Zhou,⁶⁵ the IR intensities (I_s) for the four observed modes for the trans isomer were concluded to be in the order I_2 (NO stretching) > I_3 (NN stretching) > I_1 (BN stretching) > I_4 (in-plane bending). This experimental ordering is well reproduced for the trans isomer using the CCSD(T) level of theory (see Table S7 in the Supporting Information), even within the double harmonic approximation.

I. Anharmonic Vibrational Frequencies and Isotopic Shifts. In Table 4, the fundamental vibrational frequencies for the ¹⁰B¹⁴N¹⁴NO isotopologue as well as the respective isotopic shifts of ¹¹B¹⁴N¹⁴NO and ¹⁰B¹⁵N¹⁵NO are presented. The anharmonic vibrational frequencies are determined via VPT2 theory using our cc-pCVTZ CCSD(T) quartic force field. For the ¹⁰B¹⁴N¹⁴NO trans isotopologue, the deviations between theoretical harmonic and experimental fundamental frequencies of the four modes are +85, +50, +28, and +11 cm⁻¹, respectively. On the other hand, the corresponding differences between theoretical anharmonic and experimental fundamental frequencies for the trans isomer are +36, +28, -6, and -15 cm⁻¹. The improvement in the agreement with

Table 3. Theoretical Predictions of the Total Energy, Harmonic Vibrational Frequencies, And Zero-Point Vibrational Energy For the $^2A'$ Cyclic, Trans, Cis, TS1, and TS2 $^{11}B^{14}N^{14}NO$ Molecule at the aug-cc-pVQZ CCSD(T) Level of Theory^a

| structure | total energy | $\omega_1(a')$ | $\omega_2(a')$ | $\omega_3(a')$ | $\omega_4(a')$ | $\omega_5(a')$ | $\omega_6(a'')$ | ZPVE |
|-----------|--------------|----------------|----------------|----------------|----------------|----------------|-----------------|--------|
| cyclic | -209.134170 | 1712 | 1298 | 1013 | 859 | 517 | 511 | 8.45 |
| trans | -209.128591 | 1876 | 1544 | 874 | 646 | 149 | 137 | 7.30 |
| cis | -209.111697 | 1641 | 1368 | 1011 | 679 | 189 | 85 | 7.11 |
| TS1 | -209.111462 | (1675) | (1420) | (990) | (651) | (204) | (100 <i>i</i>) | (7.06) |
| TS2 | -209.102719 | 1866 | 1234 | 1005 | 431 | 348 | 691 <i>i</i> | 6.98 |

^a Total energy is in hartree, harmonic vibrational frequency (ω) is in cm^{-1} , and ZPVE is in kcal mol^{-1} . For TS1, the total energy is the single-point energy with cc-pVQZ CCSD(T) optimized geometry, and harmonic vibrational frequencies and ZPVE are computed at the cc-pVQZ CCSD(T) level.

Table 4. Fundamental Vibrational Frequencies for the BNNO Molecule and the Corresponding Shifts upon Isotopic Substitution at the cc-pCVTZ CCSD(T) Level of Theory^a

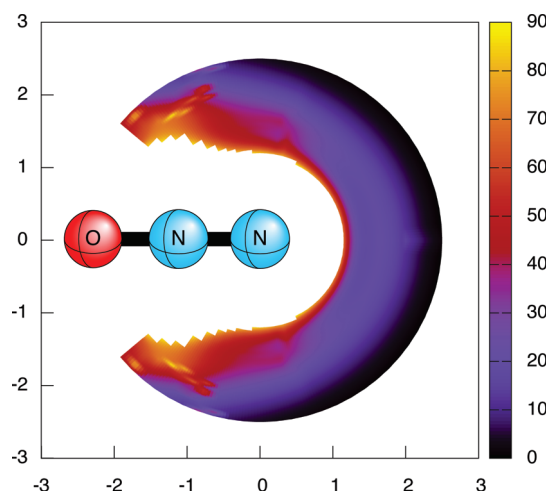
| mode (sym.) | $\nu_{10}B^{14}N^{14}NO$ | $\Delta(\nu_{11}B^{14}N^{14}NO)$ | $\Delta(\nu_{10}B^{15}N^{15}NO)$ |
|-------------------------|--------------------------|----------------------------------|----------------------------------|
| Experiment ^b | | | |
| B–N stretch | 1837 | 41 | 28 |
| N–O stretch | 1502 | 2 | 26 |
| N–N stretch | 838 | 1 | 23 |
| bending | 634 | 7 | 9 |
| Trans BNNO | | | |
| B–N stretch | 1873 | 41 | 30 |
| N–O stretch | 1530 | 2 | 27 |
| N–N stretch | 832 | 1 | 22 |
| bending | 619 | 8 | 10 |
| Cyclic BNNO | | | |
| B–N stretch | 1305 | 28 | 19 |
| N–O stretch | 1684 | 15 | 34 |
| N–N stretch | 982 | 18 | 16 |
| bending | 830 | 6 | 16 |

^a Fundamental vibrational frequencies are in cm^{-1} , and the corresponding shifts are denoted as Δ . The experimental results are shown for comparison purposes. ^b Ref 26.

inclusion of theoretical anharmonic effects is evident. However, the disagreement between experiment is unusually large for such a reliable level of theory. Of course, the theoretical results are directly comparable only to gas-phase experiments, not matrix isolation results.

From the experimental observations, the 1837 cm^{-1} transition exhibits the largest isotopic shift for ^{11}B (41 cm^{-1}) and ^{15}N (28 cm^{-1}), since it is primarily a B–N stretching mode. The 1502 cm^{-1} frequency shows a very small ^{11}B shift (2 cm^{-1}) but quite a large nitrogen isotopic shift (26 cm^{-1}), consistent with its assignment as the N–O stretching mode. The 838 cm^{-1} absorption shows almost no change among boron isotopes but exhibits a large nitrogen isotopic shift (23 cm^{-1}) and is, therefore, attributed to the N–N stretching mode.

For the global minimum cyclic isomer, the B–N stretching mode exhibits a large B isotopic shift (28 cm^{-1}) and a N isotopic shift (19 cm^{-1}). In the case of the trans isomer, the N–O and N–N stretching modes have almost no shift within B isotopes but quite large N isotopic shifts (27 and 22 cm^{-1} for the N–O and N–N stretches, respectively). Our frequency shifts upon isotopic substitution for the trans isomer are in good agreement with the experimentally observed values, in contrast to those for the cyclic global minimum; this indicates that the trans isomer was observed in the experiment.

**Figure 5.** PES (in kcal mol^{-1} and \AA units) describing the B (2P_u) + NNO ($\tilde{X}^1\Sigma^+$) (linear) reaction at the cc-pVDZ CASSCF (7, 7) level of theory. See text for details.

J. Trans or Cyclic Structure? Our theoretical investigation clearly shows that the cyclic isomer is the global minimum, but the vibrational frequencies and isotopic shifts thereof provide compelling evidence for the experimental observation of the trans isomer. To gain some insight into the conformational preferences of the reaction, we constructed a two-dimensional energetic contour plot with respect to the boron-atom position, constraining the NNO moiety to its isolated ($\tilde{X}^1\Sigma^+$) geometry and enforcing planarity. The cc-pVDZ CASSCF method with a (7, 7) active space was used in order to describe the various bonding schemes encountered on the resulting PES, which is shown in Figure 5. The area in the immediate vicinity of the molecule is repulsive within the constraints imposed, but crucially the region around the N terminus is less repulsive than that around the central nitrogen atom, favoring the formation of trans over cyclic BNNO. This feature may be explained from the NNO molecular orbitals shown in the Supporting Information, Figure S6. The 7σ MO of NNO mainly consists of the lone-pair orbital of the terminal N atom. The electropositive B atom, therefore, may be prone to approach the electron-rich terminal N atom along the NNO molecular axis.

Clearly, as the reaction proceeds, the NNO angle must decrease, so an analogous plot was generated (Figure 6) with the NNO geometry chosen as [$r_e(\text{NO}) = 1.30\text{ \AA}$, $r_e(\text{NN}) = 1.20\text{ \AA}$, $\theta_e = 123.0^\circ$] to represent a compromise between the NNO geometries adopted in the cyclic and trans isomers. The relaxation of the NNO unit changes the qualitative nature

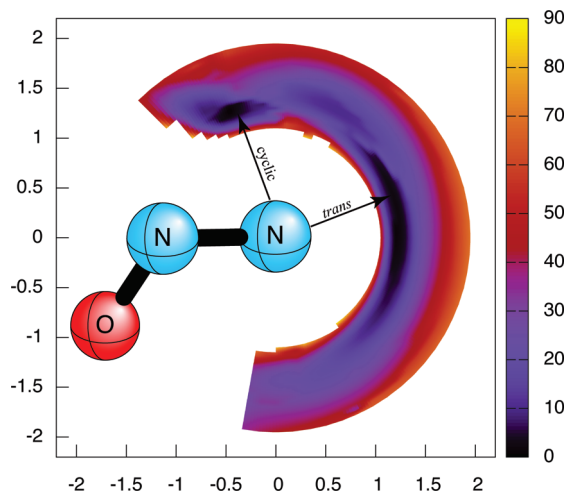


Figure 6. PES (in kcal mol⁻¹ and Å units) describing the B (²P_u) + NNO (\tilde{X}^1A') (bent) reaction at the cc-pVDZ CASSCF (7, 7) level of theory. Wells corresponding to cyclic and trans BNNO minima are labeled. See text for details.

of the potential, introducing two bound minima. The minimum corresponding to the cyclic structure, although deeper than the trans minimum, has a relatively small area, which translates into a relatively low capture cross section for boron atoms leading to cyclic BNNO formation. Although this analysis is quite crude, it offers insight into the basins of attraction on the B + NNO PES.

Concluding Remarks

Ab initio molecular electronic structure theory has been employed in order to investigate the cyclic, trans, and cis isomers of BNNO and the two isomerization reactions connecting them. At our highest level of theory, aug-cc-pVQZ CCSD(T), the trans isomer was predicted to be 3.5 kcal mol⁻¹ (2.4 kcal mol⁻¹ with the ZPVE correction) higher than the cyclic minimum. The barrier height for the uphill isomerization reaction (cyclic → trans) is determined to be 19.7 (18.3) kcal mol⁻¹. The trans and cis isomers are separated by 10.6 (10.4) kcal mol⁻¹ with a barrier (trans → TS1 → cis) of 10.8 (10.4) kcal mol⁻¹, which indicates that the trans → cis isomerization reaction is unlikely to occur in an argon matrix. Theoretically computed harmonic and anharmonic vibrational frequencies and associated IR intensities are consistent with the experimental observation of trans BNNO in an argon matrix. The dissociation energies (with ZPVE corrections) associated with BNNO (\tilde{X}^2A') → B (²P_u) + NNO ($\tilde{X}^1\Sigma^+$) for the cyclic, trans, and cis isomers were predicted to be 39.7, 37.3, and 27.0 kcal mol⁻¹, while the diatomic fragment dissociation energies BNNO (\tilde{X}^2A') → BN ($X^3\Pi$) + NO ($X^2\Sigma^+$) for the three isomers were determined to be 50.7, 48.4, and 38.0 kcal mol⁻¹, respectively. Therefore, the three equilibrium structures are well below the dissociation limits to [B (²P_u) + NNO ($\tilde{X}^1\Sigma^+$)] and [BN ($X^3\Pi$) + NO ($X^2\Sigma^+$)]. There are no bonding regions with the NNO fragment constrained (linear) to its native geometry; its geometry must relax for the B (²P_u) + NNO ($\tilde{X}^1\Sigma^+$) association to proceed. Two distinct bonding regions are found on the relaxed (bent) surface. The first

leads to formation of the trans isomer, this region being much broader but less deep than that leading to formation of cyclic BNNO. The larger capture cross section due to the broader trans well appears to explain the experimental observation of only the higher energy trans isomer.

Acknowledgment. The authors would like to thank Dr. Partha P. Bera, Dr. Justin M. Turney, and Dr. Steven E. Wheeler for insightful discussions and technical expertise. This research was supported by the Department of Energy, Basic Energy Sciences, Division of Chemical Sciences, Fundamental Interactions Team, grant no. DEFG02-97-ER14748. This research used the resources of the National Energy Research Scientific Computing Center (NERSC), supported by the Office of Science of the U.S. Department of Energy under contract no. DE-AC02-05CH11231 and the VMD software developed by the Theoretical and Computational Biophysics Group in the Beckman Institute for Advanced Science and Technology at the University of Illinois at Urbana–Champaign.

Supporting Information Available: Electron configurations, CASSCF wave functions, molecular orbitals, dissociation energies, harmonic and fundamental vibrational frequencies, total energies, dipole moments, and IR intensities of the stationary points of BNNO at various levels of theory. This material is available free of charge via the Internet at <http://pubs.acs.org>.

References

- (1) Nohl, U.; Olbrich, G. *Gmelin Handbook of Inorganic Chemistry*; Springer: Berlin, Germany, 1988.
- (2) Paine, R. T.; Narula, C. K. *Chem. Rev.* **1990**, 90, 73.
- (3) Wang, Z.; Li, S.; Zhang, L.; Sheng, Z.; Yu, S. *Propellants, Explos., Pyrotech.* **2004**, 29, 160.
- (4) Kuo, K.; Pein, R. *Combustion of Boron-Based Solid Propellants and Solid Fuels*; CRC Press: Boca Raton, FL, 1993.
- (5) Chen, D. M.; Luh, S. P.; Liu, T. K.; Wu, G. K.; Perng, H. C. *Combustion of Boron-Based Solid Propellants and Solid Fuels* **1993**, 375.
- (6) Eckl, W.; Eisenreich, N.; Menke, K.; Rohe, T.; Weiser, V. Combustion phenomena of boron containing propellants. Proceedings of the 26th International Annual Conference of ICT, Karlsruhe, Federal Republic of Germany, July 4–7, 1995; p 70.
- (7) Ritter, D.; Weisshaar, J. C. *J. Phys. Chem.* **1990**, 94, 4907.
- (8) Plane, J. M. C.; Rollason, R. J. *J. Chem. Soc., Faraday Trans.* **1996**, 92, 4371.
- (9) Clemmer, D. E.; Honma, K.; Koyano, I. *J. Phys. Chem.* **1993**, 97, 11480.
- (10) Matsui, R.; Senba, K.; Honma, K. *J. Phys. Chem.* **1997**, 101, 179.
- (11) Campbell, M. L.; McClean, R. E. *J. Phys. Chem.* **1993**, 97, 7942.
- (12) Campbell, M. L. *J. Chem. Phys.* **1996**, 104, 7515.
- (13) Campbell, M. L.; Kölsch, E. J.; Hooper, K. L. *J. Phys. Chem.* **2000**, 104, 11147.

- (14) Campbell, M. L. *J. Phys. Chem.* **2003**, *107*, 3048.
- (15) Armentrout, P. B.; Halle, L. F.; Beauchamp, J. L. *J. Chem. Phys.* **1982**, *76*, 2449.
- (16) Futerko, P. M.; Fontijn, A. *J. Chem. Phys.* **1991**, *95*, 8065.
- (17) Delabie, A.; Vinckier, C.; Flock, M.; Pierloot, K. *J. Phys. Chem.* **2001**, *105*, 5479.
- (18) Stirling, A. *J. Am. Chem. Soc.* **2002**, *124*, 4058.
- (19) Tishchenko, O.; Vinckier, C.; Nguyen, M. T. *J. Phys. Chem.* **2004**, *108*, 1268.
- (20) Tishchenko, O.; Vinckier, C.; Ceulemans, A.; Nguyen, M. T. *J. Phys. Chem.* **2005**, *109*, 6099.
- (21) Lavrov, V. V.; Blagojevic, V.; Koyanagi, G. K.; Orlova, G.; Bohme, D. K. *J. Phys. Chem.* **2004**, *108*, 5610.
- (22) Blagojevic, V.; Orlova, G.; Bohme, D. K. *J. Am. Chem. Soc.* **2005**, *127*, 3545.
- (23) Michelini, M. D. C.; Russo, N.; Alikhani, M. E.; Silvi, B. *J. Comput. Chem.* **2005**, *26*, 1284.
- (24) Palopoli, S. F.; Brill, T. B. *Combust. Flame* **1991**, *87*, 45.
- (25) Brill, T. B.; Brush, P. J.; Patil, D. G. *Combust. Flame* **1993**, *94*, 70.
- (26) Wang, G.; Zhou, M. *Chem. Phys. Lett.* **2007**, *342*, 90.
- (27) Dunning, T. H. *J. Chem. Phys.* **1989**, *90*, 1007.
- (28) Woon, D. E.; Dunning, T. H. *J. Chem. Phys.* **1993**, *98*, 1358.
- (29) Knowles, P. J.; Werner, H.-J. *Chem. Phys. Lett.* **1985**, *115*, 259.
- (30) Werner, H.-J.; Knowles, P. J. *J. Chem. Phys.* **1985**, *82*, 5053.
- (31) Hampel, C.; Peterson, K. A.; Werner, H.-J. *Chem. Phys. Lett.* **1992**, *190*, 1.
- (32) Watts, J. D.; Gauss, J.; Bartlett, R. J. *Chem. Phys. Lett.* **1992**, *200*, 1.
- (33) Raghavachari, K.; Trucks, G. W.; Pople, J. A.; Head-Gordon, M. *Chem. Phys. Lett.* **1989**, *157*, 479.
- (34) Watts, J. D.; Gauss, J.; Bartlett, R. J. *J. Chem. Phys.* **1993**, *98*, 8718.
- (35) Stanton, J. F. *Chem. Phys. Lett.* **1997**, *281*, 130.
- (36) Werner, H.-J.; Knowles, P. J.; Lindh, R.; Manby, F. R.; Schütz, M. *MOLPRO*, version 2006.1; University College Cardiff Consultants Limited: Wales, U.K., 2006.
- (37) Stanton, J. F.; Gauss, J.; Watts, J. D.; Lauderdale, W. J.; Bartlett, R. J. *Int. J. Quantum Chem.* **1992**, *44* (S26), 879.
- (38) Stanton, J. F.; Gauss, J.; Watts, J. D.; Szalay, P. G.; Bartlett, R. J.; with contributions from Auer, A. A.; Bernholdt, D. E.; Christiansen, O.; Harding, M. E.; Heckert, M.; Heun, O.; Huber, C.; Jonsson, D.; Jusélius, J.; Lauderdale, W. J.; Metzroth, T.; Michauk, C.; O'Neill, D. P.; Price, D. R.; Ruud, K.; Schiffmann, F.; Tajti, A.; Varner, M. E.; Vázquez, J. ACES II; Jürgen Gauss, John F. Stanton, and Peter G. Szalay: Mainz, Germany; Austin, TX; and Budapest 112, Hungary, 1992; <http://www.aces2.de>.
- (39) Crawford, T. D.; Sherrill, C. D.; Valeev, E. F.; Fermann, J. T.; King, R. A.; Leininger, M. L.; Brown, S. T.; Janssen, C. L.; Seidl, E. T.; Kenny, J. P.; Allen, W. D. *J. Comput. Chem.* **2007**, *28*, 1610.
- (40) Lee, T. J.; Taylor, P. R. *Int. J. Quantum Chem., Symp.* **1989**, *23*, 199.
- (41) East, A. L. L.; Johnson, C. S.; Allen, W. D. *J. Chem. Phys.* **1993**, *98*, 1299.
- (42) Nielsen, H. H. *Rev. Mod. Phys.* **1951**, *23*, 90.
- (43) Mills, I. M. In *Molecular Spectroscopy: Modern Research*; Rao, K. N., Mathews, C. W., Eds.; Academic Press: New York, 1972; p 115.
- (44) Watson, J. K. G. In *Vibrational Spectra and Structure*; Durig, J. R., Ed.; Elsevier: Amsterdam, The Netherlands, 1972; Vol. 6, p 1.
- (45) Papoušek, D.; Aliev, M. R. *Molecular Vibrational-Rotation Spectra*; Elsevier: Amsterdam, The Netherlands, 1982.
- (46) Clabo, D. A.; Allen, W. D.; Remington, R. B.; Yamaguchi, Y.; Schaefer, H. F. *Chem. Phys.* **1988**, *123*, 187.
- (47) Allen, W. D.; Yamaguchi, Y.; Császár, A. G.; Clabo, D. A.; Remington, R. B.; Schaefer, H. F. *Chem. Phys.* **1990**, *145*, 427.
- (48) Aarset, K.; Császár, A. G.; Sibert, E. L.; Allen, W. D.; Schaefer, H. F.; Klopper, W.; Noga, J. *J. Chem. Phys.* **2000**, *112*, 4053.
- (49) GRENDL is a program written by Jeremiah J. Wilke to perform general numerical differentiations to high orders of electronic structure data. Center for Computational Chemistry, University of Georgia: Athens, GA.
- (50) INTDER2005 is a general program developed by Wesley D. Allen and co-workers which performs various vibrational analyses and higher-order nonlinear transformations among force field representations. Center for Computational Chemistry, University of Georgia: Athens, GA.
- (51) Allen, W. D.; Császár, A. G. *J. Chem. Phys.* **1993**, *98*, 2983.
- (52) Allen, W. D.; Császár, A. G.; Szalay, V.; Mills, I. M. *Mol. Phys.* **1996**, *89*, 1213.
- (53) Sarka, K.; Demaison, J. In *Computational Molecular Spectroscopy*; Jensen, P., Bunker, P. R., Eds.; Wiley: Chichester, U.K., 2000; p 255.
- (54) Simmonett, A. C.; Evangelista, F. A.; Allen, W. D.; Schaefer, H. F. *J. Chem. Phys.* **2007**, *127*, 014306.
- (55) Yamaguchi, Y.; Schaefer, H. F. *ANHARM*, a FORTRAN program written for VPT2 analysis; Center for Computational Chemistry, University of Georgia: Athens, GA.
- (56) Wang, F.; Harcourt, R. D. *J. Phys. Chem. A* **2000**, *104*, 1304.
- (57) Humphrey, W.; Dalke, A.; Schulten, K. *J. Mol. Graphics* **1996**, *14*, 33.
- (58) Richard, R. M.; Ball, D. W. *J. Mol. Struct.* **2007**, *806*, 113.
- (59) Karton, A.; Martin, J. M. L. *J. Chem. Phys.* **2006**, *125*, 144313.
- (60) MacKay, B. A.; Fryzuk, M. D. *Chem. Rev.* **2004**, *104*, 385.
- (61) Schaefer, H. F. *Chem. Britain* **1975**, *11*, 227.
- (62) Fukui, K. *Acc. Chem. Res.* **1981**, *14*, 363.
- (63) Schmidt, M. W.; Gordon, M. S.; Dupuis, M. *J. Am. Chem. Soc.* **1985**, *107*, 2585.
- (64) Garrett, B. C.; Redmon, M. J.; Steckler, R.; Truhlar, D. G.; Baldrige, K. K.; Bartol, D.; Schmidt, M. W.; Gordon, M. S. *J. Phys. Chem.* **1988**, *92*, 1476.
- (65) Wang, G.; Jin, X.; Chen, M.; Zhou, M. *Chem. Phys. Lett.* **2006**, *420*, 130.